Proceedings of the 39th Chinese Control Conference
July 27-29, 2020, Shenyang, China

Path Planning for Dense Drone Formation Based on Modified Artificial Potential Fields

Hang Sun[1], Juntong Qi[1], Chong Wu[2], Mingming Wang[1]

1. School of Electrical and Information Engineering, Tianjin University, Tianjin 300072, China

E-mail: sunhang@tju.edu.cn

2. EFY intelligent control Co. ltd, Tianjin 300450, China

Abstract: Unmanned aerial vehicle (UAV) formation can accomplish complex and challenging tasks more efficiently. Path planning is one of the key issues to achieve formation flight. According to the drone light show, an artificial potential field (APF)-based path planning algorithm for dense drone formation method was proposed to realize the path planning of multiple drones and multiple targets in three-dimensional space. The problem of path oscillation was solved by improving the repulsive force model. By adding the target exchange algorithm, the problem that the individual cannot reach the target when being stuck in the local optimal solution was solved. The drone's path was improved following the performance by adding constraints. Finally, the dense formation transformation of 500 drones at 2.5m spacing was achieved and actual flight experiments were carried out. The path planning method studied in this paper can be widely used in a variety of military and civil multi rotors or helicopter clusters, which has a very high practical value.

Key Words: Drones, UAV Formation, Path Planning, Artificial Potential Field Method, Drone Light Show

1 Introduction

In recent years, with the development of positioning navigation, automatic control and other technologies, the autonomous flight capability and stability of drones have been significantly improved. And drones are widely used in military and civilian fields, such as aerial photography [1], disaster detection and inspection [2], agricultural plant protection [3] and logistics [4]. With the increasing diversification of drone missions, it is difficult for a single drone to meet all the missions. Therefore, the multi-drone cooperative formation flight has quickly become a research focus. Compared with a single drone, a drone formation can make full use of resources to complete more complex and challenging tasks.

UAV formation has been studied and applied worldwide. Intel held a performance of 500 drone formations in November 2016, breaking the Guinness World Record at the time [5]. On April 29, 2018, EHang performed a show in Xi'an consisting of 1,374 drones [6], breaking Intel's record. On September 19, 2019, this record was broken by Gao Ju innovation, with the number of drones up to 2,100 [7].

The U.S. military tested a fixed-wing UAV formation called Perdix. The press release stated that a system of 103 autonomous drones performed adaptive formation flight. The published video showed that the drones met a set of predefined targets, selected a target with a collective decision, and tracked it separately. Drones also hovered in a common place, albeit at different altitudes. Unfortunately, there was no reliable literature describing specific technical solutions [8].

As for drone formation path planning, based on the Leader-Follower method, Xiangke Wang realized the planning and flight control of 21 fixed-wing UAVs [9]. This method is proven suitable for formation flight in a layered structure and it depends on the stability of the leader. Qi used Bezier curves to fit the paths of UAV formations to achieve path planning that satisfies the constraints of UAV dynamics and verified them through actual flight tests [10]. However, no specific method for autonomous planning of multiple drones was given. SPH Engineering has developed a solution for UAV light show based on flight control such as PX4. Drone Show Software is included in the solution, which can realize the path planning of the formation and the color adjustment of lighting effects [11]. The path planning of this solution is similar to the animation production, and the travel path of the drone queue needs to be adjusted manually. The degree of automation is very low. In the first drone light show in Singapore, Kevin Z used a path planning method based on dynamic feasibility and Minimum jerk trajectory [12]. Finally, the UAV formation flight with a distance of 10m was realized. But there was still a lack of swarm intelligence trajectory in planning. Gábor Vásárhelyi studied and realized the cluster flight of 30 drones [13]. The cluster was not subject to the intervention of the central control system. Each drone independently decided its own flight route. It can maintain its formation and avoid collisions in a space with obstacles. It had a high degree of autonomy. However, the exact location of each aircraft cannot be predicted.

Based on the drone light show, a method of autonomous path planning for dense drone formation was designed in the paper. Based on the improved artificial potential field method, a path planning algorithm for drone formation was proposed. The waypoints were effectively constrained to improve the path following performance, and the contradiction between the safe distance of the drones and the path oscillation is effectively solved. The problem that the drone falls into the local optimal solution and the target is unreachable is solved by the target exchange algorithm. The path planning method studied in this paper has been used in actual flight, and can be widely used in various military and civil UAV formations in the future, with a high practical value.

*This work is supported by National Natural Science Foundation (NNSF) of China under Grant 61873182.

2 Establishment of Problem Model

The problem model of the method described in this paper is based on the drone light show performance. The performance mainly consists of the following processes:

- Formations take off in a specific order.
- Maintain formation, and moves to the performance area.
- The formation was spread out and turned into the first performance pattern.
- Change the formation to become the next pattern。
- After all performance patterns are over, return to the initial formation.
- Keep in formation and return to takeoff position.

The process is shown in Figure 1.

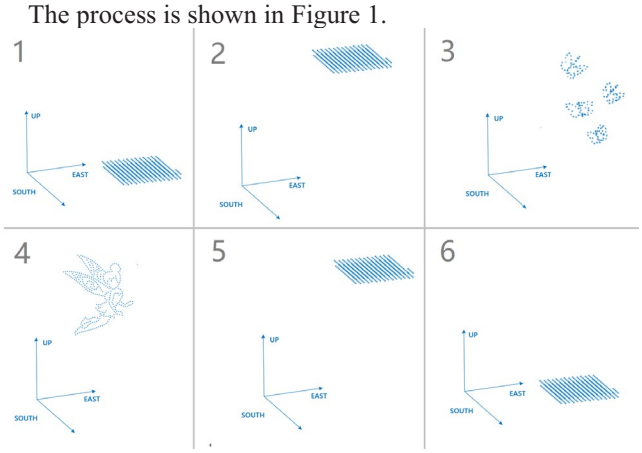

Fig. 1: The Performance Process

During the entire process, since the positions of the drones in step 2-3-4-5 are scattered and not fixed, the path planning at this time is the most complicated part of the entire process. Therefore, a problem model is established based on this step.

Establishing a spatial rectangular coordinate system: W. The three axes x_W, y_W, z_W of W are pointing east, south and sky respectively in meters.

Assuming a total of n drones, the initial formation position of the drone formation is expressed as:

$$S = [S_1, S_2, S_3, \cdots, S_i, \cdots, S_n]$$

The final position of the drone formation is expressed as:

$$E = [E_1, E_2, E_3, \cdots, E_i, \cdots, E_n]$$

The position of the drone formation at a certain time t is expressed as:

$$M_t = [M_{t1}, M_{t2}, M_{t3}, \cdots, M_{ti}, \cdots, M_{tn}]$$

Among them, S_n, E_n, and M_{tn} are the positions in W.

Therefore, the goal of the drones is to change the formation from S to E.

Assume that during the entire formation change, p path points are planned. Then all the paths of the drone formation in the process can be expressed as:

$$M = \begin{bmatrix} M_1 \\ M_2 \\ \vdots \\ M_p \end{bmatrix} = \begin{bmatrix} M_{11}, M_{12}, M_{13}, \cdots, M_{1n} \\ M_{21}, M_{22}, M_{23}, \cdots, M_{2n} \\ \vdots \quad \vdots \quad \vdots \quad \vdots \\ M_{p1}, M_{p2}, M_{p3}, \cdots, M_{pn} \end{bmatrix}$$

S, E and M are shown in Figure 2.

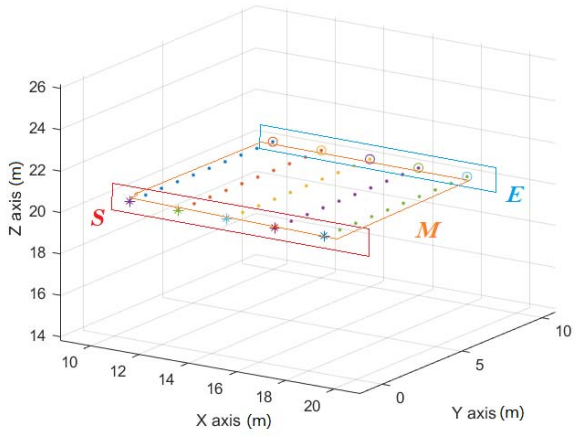

Fig. 2: All Path Points

3 Path Planning Algorithm

3.1 Introduction to Artificial Potential Field Method

Artificial potential field method is a path planning method of manipulator and mobile robot proposed by O. Khatib[14]. The algorithm pioneered the use of a virtual force field to control the robot's direction in space. The basic idea of the algorithm is:

- Determine the coordinate position of the robot, target point, and obstacle: $R, G, O_1, O_2, \cdots O_n$.
- Construct the gravitational field of the target point to the robot. The gravity of the gravitational field increases with the distance between the robot and the target point.

$$U(G) = \frac{1}{2}\varepsilon \|G - R\|^2 \quad (1)$$

Among them, $U(G)$ is the gravitational field, ε is the gravitational coefficient.

- Constructing the obstacle's repulsion field to the robot.

$$U(O_n) = \begin{cases} \frac{1}{2}\eta\left(\frac{1}{\|O_n - R\|} - \frac{1}{\rho}\right)^2, & \|O_n - R\| \le \rho \\ 0, & \|O_n - R\| > \rho \end{cases} \quad (2)$$

Among them, $U(O)$ is the repulsion field, η is the repulsion coefficient, ρ is the distance affected by obstacles. If there are multiple obstacles, the total repulsive force field is the sum of the repulsive force fields of each obstacle.

$$U(O)_{sum} = U(O_1) + U(O_2) + \cdots + U(O_n) \quad (3)$$

- Move the robot unit distance according to the direction of the resultant force to calculate the next path point. The resultant force of the robot is the derivative of the resulting force field at the robot's current position.

$$F(R) = -\nabla U(R) \quad (4)$$

- Calculate the path points until the robot reaches the end point, and the path planning is completed. Figure 3 is a schematic diagram of path planning by artificial potential field method. The solid surface is a potential field model, and the yellow points are the robot path points.

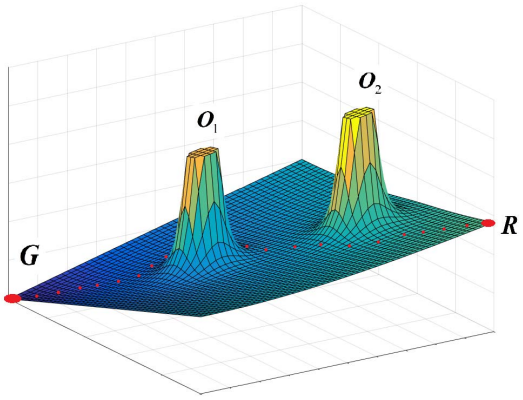

Fig. 3: Schematic Diagram of Artificial Potential Field

3.2 Algorithm Extension in 3D Multi-UAV Scene

This paper needs to apply the traditional artificial potential field method to the drone formation scenario. Drone formations fly in three-dimensional space, and there are respective starting and ending points for each drone described above. For a single drone, it is necessary to maintain a certain safety distance from other drones in the formation, so other drones can be regarded as obstacles, and the repulsive force of the obstacles affects the distance to this safety distance. In order to save computing time, in the improved algorithm, the force field is no longer calculated, and the gravitational and repulsive forces are directly calculated and then added. The extended algorithm flow is:

- Determine start formation $\boldsymbol{S}$ and end formation $\boldsymbol{E}$.
- Determine current drone position:

$$\boldsymbol{M}_1 = \begin{bmatrix} \boldsymbol{M}_{11} = \boldsymbol{S}_1 \\ \boldsymbol{M}_{12} = \boldsymbol{S}_2 \\ \vdots \\ \boldsymbol{M}_{1n} = \boldsymbol{S}_n \end{bmatrix} \tag{5}$$

- Select drone 1 to determine the starting position $\boldsymbol{M}_{11}$ and ending position $\boldsymbol{E}_1$.
- Calculate the gravitational force of the end position $\boldsymbol{E}_1$ to the current position of drone 1.

$$\boldsymbol{F}_{att}(\boldsymbol{G}) = \varepsilon(\boldsymbol{E}_1 - \boldsymbol{M}_{11}) \tag{6}$$

Set the gravitational coefficient ε=5 based on experience values.

- Calculate the distance between other drones and drone 1, and select the drone whose distance is less than the distance affected by the repulsive force. And calculate the sum of the repulsive forces separately.

$$\boldsymbol{F}_{rep}(\boldsymbol{O}_n) = \begin{cases} \eta\left(\dfrac{1}{(\boldsymbol{M}_{11}-\boldsymbol{O}_n)} - \dfrac{1}{\rho}\right)\dfrac{1}{(\boldsymbol{M}_{11}-\boldsymbol{O}_n)^2}\cdot \\ \qquad \nabla(\boldsymbol{M}_{11}-\boldsymbol{O}_n), \|\boldsymbol{O}_n - \boldsymbol{R}\| \le \rho \\ 0 \qquad , \|\boldsymbol{O}_n - \boldsymbol{R}\| > \rho \end{cases} \tag{7}$$

$$\boldsymbol{F}_{rep}(\boldsymbol{O})_{sum} = \boldsymbol{F}_{rep}(\boldsymbol{O}_1) + \boldsymbol{F}_{rep}(\boldsymbol{O}_2) + \cdots + \boldsymbol{F}_{rep}(\boldsymbol{O}_n) \tag{8}$$

In order to ensure the safe distance between the drones, so that the drones cannot fly into the repulsive force field of other drones, the repulsive strength should be far greater than the gravity, set the coefficient of repulsion $\eta = 200$.

- The gravitational repulsive force is added to determine the next moving direction of the drone according to the resultant force. Moving a certain distance in this direction is the next waypoint for this drone.

$$\boldsymbol{F}_{sum} = \boldsymbol{F}_{rep}(\boldsymbol{O})_{sum} + \boldsymbol{F}_{att}(\boldsymbol{G}) \tag{9}$$

$$\boldsymbol{M}_{21} = \boldsymbol{M}_{11} + \boldsymbol{l}\cdot\boldsymbol{F}^*_{sum} \tag{10}$$

Among them, $\boldsymbol{l}$ is moving distance, $\boldsymbol{F}^*_{sum}$ is normalized resultant force vector.

- Repeat steps 3-6, select drones 2-$\boldsymbol{n}$ and follow the same steps to calculate $\boldsymbol{M}_{22}$ - $\boldsymbol{M}_{2n}$,get $\boldsymbol{M}_2$.
- Check if there is a drone in $\boldsymbol{M}_n$ that has reached the distance $\boldsymbol{l}$ near the target point in the target formation $\boldsymbol{E}$. If it exists, determined that the drone reaches the target point, and moves to the target point and stay.
- Repeat steps 2-8, calculate drone formation position $\boldsymbol{M}_3, \boldsymbol{M}_4, \boldsymbol{M}_5, \cdots$. When calculated

$$\boldsymbol{M}_p = \boldsymbol{E} \tag{11}$$

Judging that all drones have reached the target location in step $\boldsymbol{P}$, the entire path planning ends.

3.3 Drone Dynamic Constraint in Path Planning

Due to the objective physical properties of drones, there are limits to maximum speed and acceleration. Therefore, in path planning, more reasonable path points need to be planned to satisfy the limited performance of the drones. In this paper, the maximum speed of the drone is $3\boldsymbol{m}/\boldsymbol{s}$, the maximum acceleration of the drone is $3\boldsymbol{m}/\boldsymbol{s}^2$, waypoints follow frequency at 25 per second.

In the algorithm described in this paper, the parameter that constrains the maximum speed and maximum acceleration is the single-step moving distance $\boldsymbol{l}$. Assuming that $\boldsymbol{l}$ is a constant value, a large acceleration will occur when the drone starts and ends its movement, which will adversely affect flight safety. So, we need to find a way to control the size of $\boldsymbol{l}$ reasonably.

In the process of path following by the drone, the faster the drone is, the worse the path following accuracy is, so the smaller the distance between the drones, the lower the speed should be to ensure safety. The size of $\boldsymbol{l}$ can be determined based on the distance from the drone to the starting point, the distance between other drones and the target point. Assuming that the path points of the drone $\boldsymbol{i}$ is being calculated at this time, then:

$$\boldsymbol{D}_{R_iS_i} = \|\boldsymbol{R}_i - \boldsymbol{S}_i\| \tag{12}$$

$$\boldsymbol{D}_{R_iE_i} = \|\boldsymbol{R}_i - \boldsymbol{E}_i\| \tag{13}$$

$$\boldsymbol{D}_{R_iO} = \boldsymbol{Min}\|\boldsymbol{R}_i - \boldsymbol{O}_j\|, \boldsymbol{j} = 1,2,\cdots,\boldsymbol{n} \tag{14}$$

$$\boldsymbol{l} = \frac{\boldsymbol{Min}(\boldsymbol{D}_{R_iS_n}, \boldsymbol{D}_{R_iE_i}, \frac{\boldsymbol{D}_{R_iO}}{2})}{25} \tag{15}$$

Among them, $\boldsymbol{D}_{R_iS_i}$ is the distance from the drone to the starting point, $\boldsymbol{D}_{R_iE_i}$ is the distance from the drone to the end point, $\boldsymbol{D}_{R_iO}$ is the minimum distance from the drone to other drones. The minimum value of $\boldsymbol{l}$ is 0 and the maximum

value is 0.12. That is, the minimum speed of the drone is $0\boldsymbol{m}/\boldsymbol{s}$, and the maximum speed is $3\boldsymbol{m}/\boldsymbol{s}$. According to the formula, the distance-velocity relationship between the drone and the starting point and the target point is:

$$0\boldsymbol{m}-3\boldsymbol{m}\rightarrow 0\boldsymbol{m}/\boldsymbol{s}-3\boldsymbol{m}/\boldsymbol{s}$$

The relationship between minimum drone distance -velocity is:

$$0\boldsymbol{m}-6\boldsymbol{m}\rightarrow 0\boldsymbol{m}/\boldsymbol{s}-3\boldsymbol{m}/\boldsymbol{s}$$

Because of $\boldsymbol{D}_{R_iS_i}$, $\boldsymbol{D}_{R_iE_i}$ and $\boldsymbol{D}_{R_iO}$ do not change abruptly, the speed change of the drone is also relatively continuous, and the maximum acceleration is less than $3\boldsymbol{m}/\boldsymbol{s}^2$.

3.4 Path Smoothing

In actual path planning, a drone will pop up immediately after entering the repulsive field, and then re-enter the repulsive field under the action of gravity, resulting an oscillating path, as shown in the figure 4.

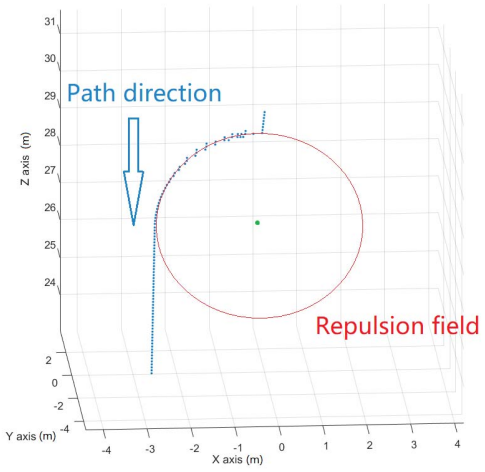

Fig. 4: Oscillating Path

As mentioned above, in order to ensure the distance between the drones, the repulsion coefficient η >> gravity coefficient ε. As a result, the force of the repulsive field on the drone is much greater than the gravitational force, and the direction of the force on the drone will change suddenly at the boundary of the repulsive field. Therefore, the repulsive force field needs to be reconstructed.

$$\boldsymbol{U}(\boldsymbol{O}_n)=\begin{cases}\frac{1}{2}\eta_1\left(\frac{1}{\|\boldsymbol{O}_n-\boldsymbol{R}\|}-\frac{1}{\rho_2}\right)^2, & \|\boldsymbol{O}_n-\boldsymbol{R}\|\le\rho_1\\ \frac{1}{2}\eta_2\left(\frac{1}{\|\boldsymbol{O}_n-\boldsymbol{R}\|}-\frac{1}{\rho_2}\right)^2, & \rho_1<\|\boldsymbol{O}_n-\boldsymbol{R}\|\le\rho_2\\ 0, & \|\boldsymbol{O}_n-\boldsymbol{R}\|>\rho_2\end{cases}\quad(16)$$

The new repulsive force field is divided into two layers. Outer repulsive force coefficient η_1=5, inner repulsive force coefficient η_2=200, outer influence distance ρ_2=3.5$\boldsymbol{m}$, inner influence distance ρ_1=2.5$\boldsymbol{m}$. The outer repulsion coefficient and the gravitational coefficient are in the same order of magnitude. Therefore, when the drone flies into the outer repulsion field, the force is small and the direction of the drone changes slowly. The inner repulsive force field can still ensure the minimum safe distance between the drones. This method effectively solves the problem of path oscillation. As shown in Figure 5.

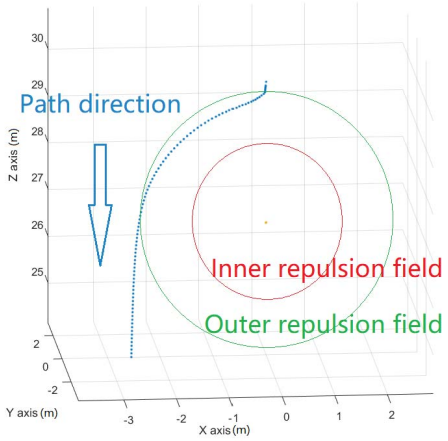

Fig. 5: Smooth Path

3.5 Target Exchange Algorithm

When there are other drones densely around the target point especially when the drones have reached their respective target points, under the influence of multiple repulsive forces and target gravity, it is possible to form a local optimal solution, leading to the current drone unable to reach the target point and was "blocked" between multiple obstacle drones. As shown in Figure 6.

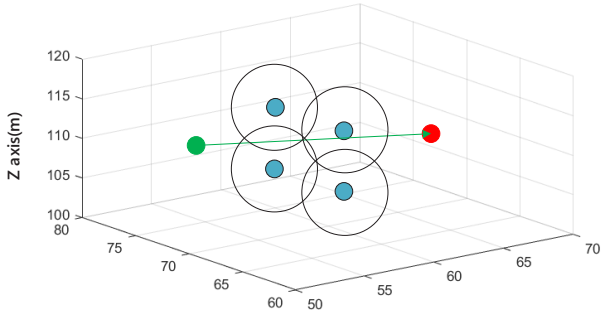

Fig. 6: The “Blocked”

The background of this article is the formation of homogeneous drone formation. The functions of the drones can be replaced with each other. When this happens, if the "blocked" drone can be exchanged with the "blocked" drone's target point, can solve the local optimal solution without affecting the functional requirements of the formation.

The conditions for judging drone target exchange are as follows:

- Drone $\boldsymbol{d}$ enters the repulsive field range of at least two other drones that have reached the end position. Assume that other drones are $\boldsymbol{a}_1,\boldsymbol{a}_2,\cdots,\boldsymbol{a}_n$, and the current path planning waypoints are $\boldsymbol{k}$, that is:

$$\begin{gathered}\exists\left(\left\|\boldsymbol{M}_{ka_1}-\boldsymbol{M}_{kd}\right\|<\rho_2\right)\wedge\left(\boldsymbol{M}_{ka_1}=\boldsymbol{E}_{a_1}\right)\\ \vdots\\ \left(\left\|\boldsymbol{M}_{ka_n}-\boldsymbol{M}_{kd}\right\|<\rho_2\right)\wedge\left(\boldsymbol{M}_{ka_n}=\boldsymbol{E}_{a_n}\right),\boldsymbol{n}\ge 2\end{gathered}\quad(17)$$

- At least one drone that generates repulsive force is located between drone $\boldsymbol{d}$ and target point $\boldsymbol{E}_d$. Assuming the drone that match this condition is $\boldsymbol{b}_1,\boldsymbol{b}_2,\cdots,\boldsymbol{b}_n$, then:

$$\begin{aligned} &\exists\left\|\boldsymbol{M}_{kb_1}-\boldsymbol{E}_d\right\|<\left\|\boldsymbol{M}_{kd}-\boldsymbol{E}_d\right\|,\\ &\quad\vdots\\ &\left\|\boldsymbol{M}_{kb_n}-\boldsymbol{E}_d\right\|<\left\|\boldsymbol{M}_{kd}-\boldsymbol{E}_d\right\|,\boldsymbol{n}\geq 1,\\ &\{\boldsymbol{b}_1,\boldsymbol{b}_2,\cdots\boldsymbol{b}_n\}\subseteq\{\boldsymbol{a}_1,\boldsymbol{a}_2,\cdots\boldsymbol{a}_n\}, \end{aligned} \tag{18}$$

- The distance between the current path point and the target point is greater than the previous path point and the target point of drone $\boldsymbol{d}$.

$$\left\|\boldsymbol{M}_{(k-1)d}-\boldsymbol{E}_d\right\|<\left\|\boldsymbol{M}_{kd}-\boldsymbol{E}_d\right\| \tag{19}$$

If condition (17,18,19) are true at the same time, can decide to trigger the target exchange algorithm. The method of target exchange is: among the drones that meet the condition 2, select the one closest to the drone currently trapped in the local optimal solution. Let this drone be $\boldsymbol{r}$:

$$\left\|\boldsymbol{M}_{kr}-\boldsymbol{M}_{kd}\right\|=\boldsymbol{Min}\left\|\boldsymbol{M}_{kb_i}-\boldsymbol{M}_{kd}\right\|,\ \boldsymbol{r},\boldsymbol{b}_i\in\{\boldsymbol{b}_1,\boldsymbol{b}_2,\cdots\boldsymbol{b}_n\} \tag{20}$$

Swapping the target $\boldsymbol{E}_r$ of the drone $\boldsymbol{r}$ and the target $\boldsymbol{E}_d$ of the drone $\boldsymbol{d}$ to destroy the current force field, as shown in Figure 7, the current local optimal problem can be effectively solved. The drone formation can enter the formation $\boldsymbol{E}$.

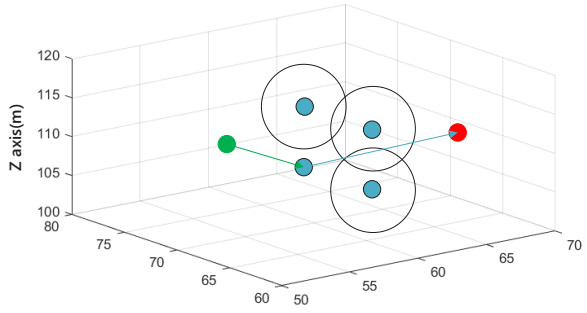

Fig. 7: Target Exchange

4 Path Planning Simulation Experiment

4.1 Experiment and Result

Based on the algorithm described above, a path planning simulation experiment was performed using 500 drones in formation. The formation changed from 3D "dancing girl" pattern $\boldsymbol{S}$ to "guitar" pattern $\boldsymbol{E}$. The effect of the pattern is shown in the figure 8 and 9.

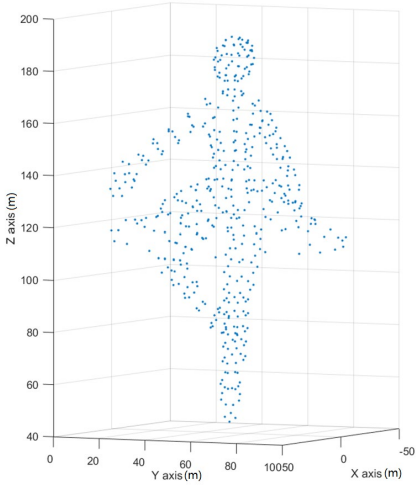

Fig. 8: Dancing Girl

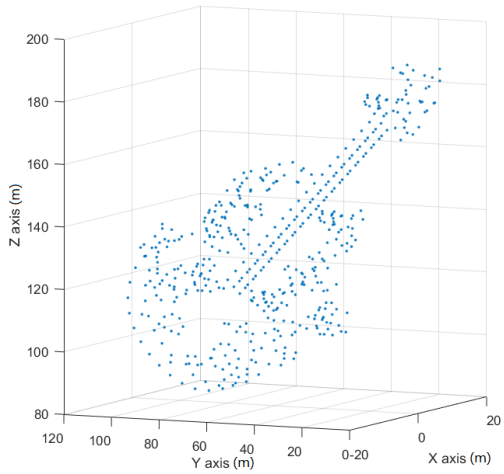

Fig. 9: Guitar

By using the path planning algorithm described above, the result is that the drone formation completed the entire path planning after 1331 cyclic iterations, with a total flight time of 53.2 seconds and triggering 13 target exchanges. The paths of all drones are shown as figure 10. The green dots are the starting formation, and the purple dots are the ending formation.

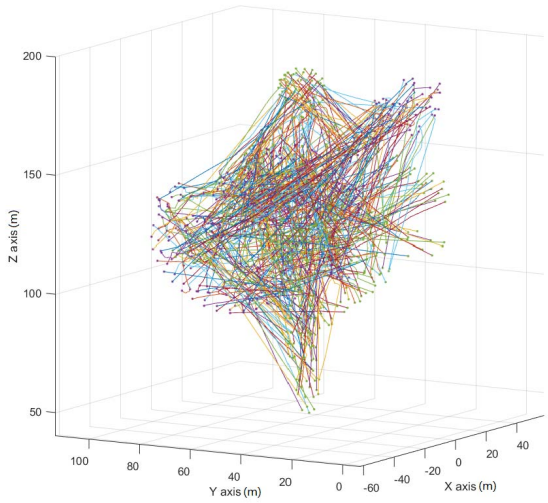

Fig. 10: All Path Points

4.2 Result Analysis

The planned path needs further verification to ensure that each drone can follow the path to fly.

Calculate the speed and acceleration of each drone in the $\boldsymbol{x},\boldsymbol{y},\boldsymbol{z}$ 3 axes direction. The speed and acceleration of 500 drones in the $\boldsymbol{x}$ axis direction is shown in Figure 11 and Figure 12. The $\boldsymbol{z}$ axis in the two figures shows the speed and acceleration of 500 drones from 1 to 1331 waypoints. The figure shows the $\boldsymbol{x}$ axis maximum speed is less than $3\boldsymbol{m}/\boldsymbol{s}$ and maximum acceleration is less than $3\boldsymbol{m}/\boldsymbol{s}^2$ .The data on the $\boldsymbol{y},\boldsymbol{z}$ axes are similar to the $\boldsymbol{x}$ axis and will not be shown for the time being.

The minimum distance between each drone at each waypoint and all other drones was calculated. After calculation, the minimum distance between the drones was $2.7\boldsymbol{m}$. As shown in Figure 13.

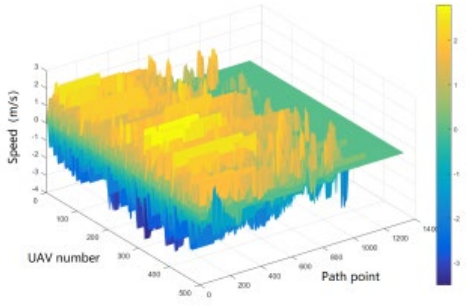

Fig. 11: X-axis Speed

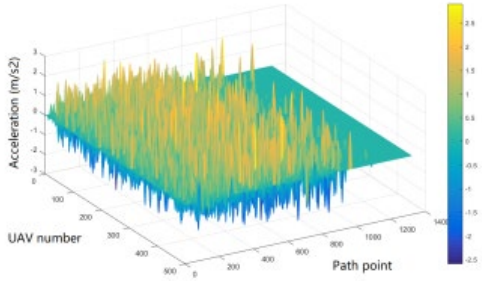

Fig. 12: X-axis Acceleration

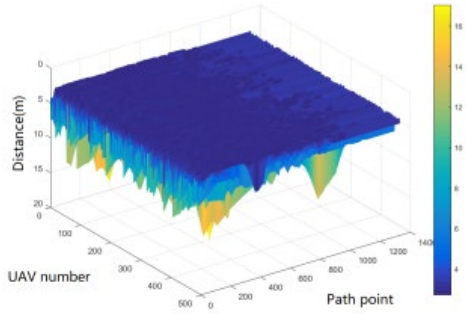

Fig. 13: Minimum Distance Between Drones

5 Verification of Actual Flight Experiments

After the path planning is implemented, flight verification is performed using an actual drone flight platform.

Formation system consists of drones, ground control station, communication equipment and RTK base station. The system structure diagram is shown in Figure 14. The system workflow is:

- Drones and other equipment placed on the flight site.
- System startup.
- Upload path via Wi-fi to drones.
- Clock synchronization using GPS timing [15].
- Give take off order.
- Drones follow the planned path.
- Land and end the flight.

Figure 15 is a real flight picture of the planned path in this paper for 500 drone formations. It can be seen that the flight effect is good, and no collision accident occurred after changing the formation. The control strategy and software structure of drone formation are not the focus of this paper, so they will not be described in detail.

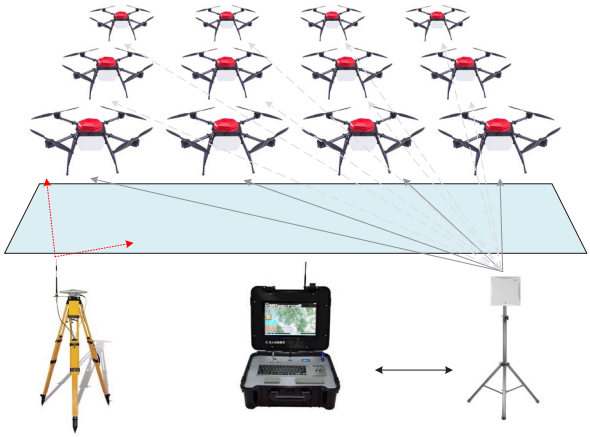

Fig. 14: System Structure

Fig. 15: Real Flight of 500 Drones

6 Conclusion

This paper realized a path planning method for dense drone formation. This method is based on the traditional artificial potential field method and realizes multi-UAV path planning in three-dimensional space by changing the algorithm structure. According to the dynamic constraints of the drones, the planning algorithm parameters are dynamically adjusted to satisfy the speed and acceleration requirements of the drone flight. By changing the structure of the repulsive force field, the problem of path oscillation is effectively solved. A target exchange algorithm for drone formation is designed to solve the problem that drones fall into the local optimal solution and cannot reach the target point during the path planning process. Finally, the path planning of the drone formation acceleration less than 3, the maximum speed less than 3, and the 2.5m spacing is realized. Through the two formations transformation and actual flight of five hundred drones formation, the feasibility of the method is verified. The path planning method studied in this paper has been used in actual flight, and can be widely used in various military and civil UAV formations in the future, with a high practical value.

References

[1] Eckert G, Cassidy S, Tian, N. Using Aerial Drone Photography to Construct 3D Models of Real World Objects in an Effort to Decrease Response Time and Repair Costs Following Natural Disasters, *Advances In Computer Vision*, CVC, VOL 1, 943: 317–325, 2020.

[2] Kim S, Lee W, Park YS, et al. Forest fire monitoring system based on aerial image, *International Conference on Information & Communication Technologies for Disaster Management*. IEEE, 2017: 1-6.

[3] SAARI, Heikki, PELLIKKA, et al. Unmanned Aerial Vehicle (UAV) operated spectral camera system for forest and agriculture applications. *Proceedings of SPIE - The International Society for Optical Engineering*, 2011, 8174(1):466-471.
[4] Song BD, Park K, Kim J. Persistent UAV delivery logistics: MILP formulation and efficient heuristic, *Computers and Industrial Engineering*, v120, June 2018: 418-428.
[5] K. Kaplan, "500 drones light night sky to set record," by Intel, 4th November 2016; https://iq.intel.com/500-drones-light-show-sets-record/.
[6] Ehang, "1374 drone formations in Xi'an City Wall won the Guinness World Record title." http://www.ehang.com/news/364.html;
[7] High Great, "World Record | High Great celebrates the 70th birthday of the motherland with 2,100 drones". http://www.hg-cm.com/product/16/82/92;
[8] US. Army, "Department of Defense Announces Successful Micro-Drone Demonstration," U.S. Department of Defense, 9 January 2017; www.defense.gov/News/News-Releases/News-Release-View/Article/1044811/department-of-defense-announcessuccessful-microdrone-demonstration/.8.
[9] Xingke W, et al, Coordinated flight control of miniature fixed-wing UAV swarms: methods and experiments, *Science China. Information Sciences*, 62(11), November 2019.
[10] Juntong Q, Tong D, et al. Design of multi-UAVs flight control system and trajectory planning. *37th Chinese Control Conference (CCC)*, 2018, 9968-9973.
[11] Drone Show Software: https://github.com/ugcs/ddc
[12] Ang, Kevin Z, et al. "High-Precision Multi-UAV Teaming for the First Outdoor Night Show in Singapore." *Unmanned Systems* (2018):1-27.
[13] Vásárhelyi Gábor, et al. "Optimized flocking of autonomous drones in confined environments." *Science Robotics* 3.20(2018): eaat3536-.
[14] Khatib, O. "Real-time obstacle avoidance for manipulators and mobile robots." *Proceedings. 1985 IEEE International Conference on Robotics and Automation IEEE, 2003*.
[15] Lewandowski, W. , J. Azoubib , and W. J. Klepczynski . "GPS: primary tool for time transfer." *Proceedings of the IEEE* 87.1(1999):163-172.